

Contents lists available at ScienceDirect

Analytica Chimica Acta

journal homepage: http://ees.elsevier.com



Ultrasensitive liposome-based assay for the quantification of fundamental ion channel properties

Yi Shen^a, Yulong Zhong^b, Fan Fei^a, Jielin Sun^c, Daniel M. Czajkowsky^{a,***}, Bing Gong^{b,**}, Zhifeng Shao^{a,*}

- ^a Bio-ID Center, School of Biomedical Engineering, Shanghai Jiao Tong University, Shanghai, 200240, China
- ^b Department of Chemistry, The State University of New York at Buffalo, Buffalo, NY, 14260, United States
- c Shanghai Center for Systems Biomedicine, Key Laboratory of Systems Biomedicine (Ministry of Education), Shanghai Jiao Tong University, Shanghai, 200240, China

ARTICLE INFO

Article history: Received 26 August 2019 Received in revised form 16 Febraury 2020 Accepted 22 March 2020 Available online xxx

Keywords
Liposome-based assay
Ion channel
Quantitative model
Ultrasensitivity

ABSTRACT

One of the most widely used approaches to characterizing transmembrane ion transport through nanoscale synthetic or biological channels is a straightforward, liposome-based assay that monitors changes in ionic flux across the vesicle membrane using pH- or ion-sensitive dyes. However, failure to account for the precise experimental conditions, in particular the complete ionic composition on either side of the membrane and the inherent permeability of ions through the lipid bilayer itself, can prevent quantifications and lead to fundamentally incorrect conclusions. Here we present a quantitative model for this assay based on the Goldman–Hodgkin–Katz flux theory, which enables accurate measurements and identification of optimal conditions for the determination of ion channel permeability and selectivity. Based on our model, the detection sensitivity of channel permeability is improved by two orders of magnitude over the commonly used experimental conditions. Further, rather than obtaining qualitative preferences of ion selectivity as is typical, we determine quantitative values of these parameters under rigorously controlled conditions even when the experimental results would otherwise imply (without our model) incorrect behavior. We anticipate that this simply employed ultrasensitive assay will find wide application in the quantitative characterization of synthetic or biological ion channels.

© 2020

1. Introduction

There is presently intense interest in the development of synthetic nano-channels with specific transport properties for a wide variety of applications, including molecular sensing, water purification, materials separation, and novel therapeutics [1–8]. Detailed functional characterization of these channels, particularly in relation to their precise spatial and dynamic structure, is one of the most essential steps for their rational development as well as for an understanding of the basic mechanisms of molecular and ion transport through pores of nanoscopic dimensions [9–20].

 $\label{lem:condition} \emph{E-mail addresses:} \ dczaj@sjtu.edu.cn (D.M. Czajkowsky); \ bgong@buffalo.edu (B. Gong); zfshao@sjtu.edu.cn (Z. Shao)$

Two of the most fundamental functional properties of any nano-channel are the ionic selectivity and permeability, and to date, although other methods have been introduced [21-27], the most commonly employed experimental technique to characterize these parameters is a simple assay based on lipid vesicles first introduced by Deamer and colleagues [28-48]. While this method can be used with a wide range of biological fluids, it is most commonly used with pure buffers as a means to quickly assess the permeability of purified channels. This assay uses liposome-entrapped fluorescent dyes that are either sensitive to changes in pH or ion concentrations to reflect the total ionic flux across the membrane. In the most common scenario where a change in pH is measured, the assay initiates with the addition of a strongly acidic or alkaline solution to the extra-vesicular solution. This generates a pH gradient across the membrane that drives the movement of both protons (H+) and hydroxide ions (OH-) across the membrane, leading to a change in the intra-vesicular pH. As described in detail below, the rate of pH change depends not only on the membrane permeability to H+ and OH-, but also to all ions present in

^{*} Corresponding author.

^{**} Corresponding author.

^{***} Corresponding author.

the solution. Thus, measurement of the time-dependent changes in fluorescence in the presence of ion-selective nanopores compared to those in their absence provides a means to determine the ion permeability of the nanopores, while measurement in the presence of different ions yields the ion selective properties of the pores. However, since the lipid membrane itself, regardless of its specific composition, is also permeable to many ionic species, these measurements only enable qualitative comparisons of permeability even for strongly selective and highly permeable channels. Further, as we show below, failure to account for the correct ionic composition on either side of the membrane can easily lead to erroneous conclusions about ionic selectivity.

Thus, there is an urgent need for a rigorous theoretical understanding of this assay, both to avoid mischaracterizations but also to maximize its precision and sensitivity, as well as to enable quantification of basic functional properties of the channels. To this end, we have examined this technique using a quantitative model based on the Goldman-Hodgkin-Katz theory [49], explicitly taking into account the ionic composition of the solution and the ion permeability of the lipid bilayer itself. Using this model, we identify generally applicable, optimal experimental conditions that increase the detection sensitivity of the permeability by 100-fold over the typically employed conditions, enabling the detection of otherwise unresolvable, weakly permeable channels as well as small differences in ion selectivity. Further, strikingly, we show that data exhibiting apparently qualitatively incorrect trends in ion selectivity nonetheless yield quantitatively correct values following analysis with our model. Overall, thus, this work describes a quantitative, highly accessible and sensitive in vitro method by which to easily obtain basic functional properties of a broad range of synthetic or purified biological nanoscopic ion channels.

2. Experimental section

2.1. Preparation of unilamellar vesicles

(LUVs) of unilamellar vesicles POPC toyl-2-oleoyl-sn-glycero-3-phosphocholine, Avanti Polar Lipids, Alabaster, AL, USA) containing the dye, HPTS (8-hydroxypyrene-1, 3, 6-trisulfonicacid, Sigma-Aldrich, St. Louis, MO, USA) [50-54] were prepared by first evaporating the POPC stock solution (chloroform) under vacuum for 1 h to remove the solvent, after which a HEPES buffer with a HPTS concentration of 0.03 mM was added to obtain a final lipid concentration of 1 mg mL⁻¹. The concentrations of HEPES, salt, and other parameters of the solution are different for different experiments, as described below. Upon dissolution in water, the pH of the HEPES solution is ~5.3, which is the initial solution pH for all experiments, unless indicated otherwise. The lipids were allowed to become fully equilibrated at room temperature for 1 h, followed by extrusion through 0.1 µm polycarbonate membrane filters (Avanti Polar Lipids, US). The size of the LUVs was subsequently measured with a dynamic light scattering (DLS) particle analyzer (Nano ZS90, Malvern, UK) and a cryo transmission electron microscope (cryo-EM) (Talos F200C G2, Thermo Fisher Scientific, US). The fluorescent dye in free solution was removed by gel filtration using a Sephadex G-50 (GE Healthcare, US) column.

2.2. Measurement of ion permeability

Gramicidin A (gA, Sigma-Aldrich, St. Louis, MO, USA) dissolved in ethanol was added to the vesicle solution, which was incubated for 5 min before the extra-vesicular pH was increased. In each experiment, the same volume of the gA solution (1 μ L to the 2 mL vesicle solution) was added to give the indicated concentration. The addition of the same volume of ethanol alone does not change the fluorescence measurements from those of the control measurements without added ethanol (data not shown). The emission of the entrapped HPTS was monitored with a fluorescence spectrometer (LS55, PerkinElmer, Hopkinton, MA, USA) with the excitation wavelength of 450 nm and emission wavelength of 510 nm. The slit width was 5 nm for both and the data acquisition interval was 0.1 s. After 500 s, the vesicles were lysed by the addition of 0.1% TritonX-100 to obtain the maximal fluorescence intensity for normalization.

2.3. The quantitative flux model

In this assay, the ion permeability is determined by monitoring the changes in the fluorescence intensity of the liposome-entrapped HPTS, whose fluorescence emission increases several-fold upon alkalization of the solution (p $K_a \sim 7$) [55–57]. Increasing the extra-vesicular pH drives the movement of H⁺ and OH⁻ across the membrane, owing to the permeability of the membrane to both H⁺ and OH⁻. This leads to the rapid generation of a transmembrane potential that counters the further movement of H⁺ and OH⁻ and leads to a small change in the pH within the vesicle at equilibrium. However, all of the ions present in the solution, not just H⁺ and OH⁻, also translocate across the membrane in response to this transmembrane potential, which allows further movement of H⁺ and OH⁻ (Fig. 1), until the pH in the vesicle reaches that of

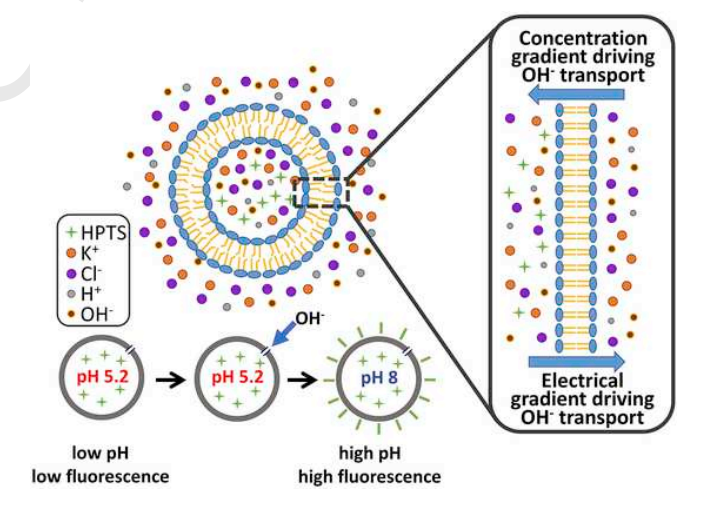


Fig. 1. Illustration of the principle underlying the liposome assay. The addition of a strongly alkaline solution to the vesicle solution drives the transmembrane movement of H^+ and OH^- ions. The movement owing to the concentration gradient produces an electrical gradient that opposes further H^+/OH^- movement. This electrical gradient also drives the trans-bilayer movement of all other ions in solution, which limits the rate at which equilibrium is achieved. Measurement of the rate at which the pH changes within the vesicle with a pH-sensitive dye (depicted in the lower panels) enables a determination of the rate of ion transport across the bilayer and thus also the ion permeability of the membrane.

the extra-vesicular solution. Because the membrane permeability of ions other than $\mathrm{H^+}$ or $\mathrm{OH^-}$ is much lower [29], the measured kinetics of fluorescence emission (reflecting the intra-vesicular pH) is mostly determined by the flow of these ions. Therefore, these kinetic measurements can be used to determine the ion transport properties of membrane-embedded channels under appropriate conditions. Moreover, when the ionic conditions are changed for the same channel, their relative ion selectivity can also be determined by these measurements.

To describe this kinetic process, we developed a quantitative flux model based on the Goldman–Hodgkin–Katz theory which includes two factors known to influence the motion of ions across a permeable membrane [49]: the difference in the ionic concentration on either side of the membrane and the transmembrane electric field. The Goldman–Hodgkin–Katz theory is derived from the Nernst–Planck equation, which is a well-established model to describe the diffusive motion of the charged particles under an electric field. In particular, the Nernst-Planck equation describes the motion of the ions owing to both the electric force and the concentration gradients, and the Goldman–Hodgkin–Katz flux equation is a solution of the Nernst-Planck equation under simplifying assumptions [49].

The ion flux, which is the number of translocated ions per unit membrane area per unit time, can be calculated as:

$$j_A = -D_A \left(\frac{d[A]}{dz} - \frac{n_A F}{RT} \frac{E_m}{L} [A] \right) \tag{1}$$

where D_A is the diffusion constant, [A] is the concentration of ion A, z is the thickness of the membrane, n_A is the charge valence, T is the temperature, R is the molar gas constant, F is the Faraday constant and E_m is the membrane potential. The first term in equation (1) corresponds to Fick's law of diffusion, which gives the flux due to diffusion down the concentration gradient. The second term is the flux due to the electric field, the Stokes-Einstein relation applied to electrophoretic mobility. The ion flux, j_A , can be re-written as:

$$j_A = \mu n_A P_A \frac{[A]_{out} - [A]_{in} e^{n\mu}}{1 - e^{n\mu}}$$
 (2)

where $\mu = \frac{FE_m}{RT}$, $P_A = \frac{D_A}{L}$ and P_A is the ionic permeability.

Considering a typical case where the salt is NaCl, the temporal evolution of the ion concentration inside the vesicle and the transmembrane electric field, E(t), can be calculated by the following:

$$\begin{split} \frac{d[Na]_{in}}{dt} &= j_{Na} \frac{S}{V} = \frac{S}{V} \mu P_{Na} \frac{[Na]_{out} - [Na]_{in} e^{n\mu}}{1 - e^{n\mu}} \\ \frac{d[Cl]_{in}}{dt} &= j_{Cl} \frac{S}{V} = -\frac{S}{V} \mu P_{Cl} \frac{[Cl]_{out} - [Cl]_{in} e^{n\mu}}{1 - e^{n\mu}} \\ \frac{d[H]_{in}}{dt} &= j_{H} \frac{S}{V} = \frac{S}{V} \mu P_{H} \frac{[H]_{out} - [H]_{in} e^{n\mu}}{1 - e^{n\mu}} \\ \frac{d[OH]_{in}}{dt} &= j_{OH} \frac{S}{V} = -\frac{S}{V} \mu P_{OH} \frac{[OH]_{out} - [OH]_{in} e^{n\mu}}{1 - e^{n\mu}} \\ E(t) &= \frac{Q}{CS} \end{split}$$
(3)

where S is the surface area of the vesicle, V is the volume of the vesicle, Q is the electric charge content inside the vesicle and C is the membrane capacitance per unit

area (\sim 0.5 μF cm $^{-2}$). The intra-vesicular and extra-vesicular [H^+] concentrations were adjusted based on the buffering of the HEPES molecule according to:

$$K_a = \frac{[HEPES^-][H^+]}{[HEPES]} \tag{4}$$

where *HEPES*⁻ is the deprotonated form of HEPES, and K_a is the dissociation constant of HEPES ($10^{-7.5}$ mol L⁻¹) appropriate for the experiments under investigation here (pH > 5) [58]. Further, the volume change of the vesicle induced by the change in salt concentration, V(t), which leads to a small change in the salt concentration inside the vesicle, is determined by:

$$\frac{dV(t)}{dt} = P_f(SAV)(MVW) \left(\frac{c_{in}}{V(t)} - c_{out}\right)$$
 (5)

where P_f is the osmotic water permeability coefficient, SAV is the vesicle surface area to volume ratio, MVW is the molar volume of water (18 cm³ mol⁻¹), and c_{in} and c_{out} are the initial concentrations of the total solute inside and outside the vesicle, respectively. We numerically calculated the changes in intra-vesicular ion concentration, the adjustments to the pH resulting from the protonation of HEPES, the resulting electric field, and the volume change for a given small time-step, Δt (here, 10^{-7} s), iteratively for the duration of the experiment. All of the calculations were carried out using Matlab (MathWork, Natick, USA) using routines that are available upon request.

3. Results and discussion

3.1. Validating the quantitative flux model

To first verify the accuracy of the quantitative flux model, we examined its predictions for an experiment using POPC vesicles free of any channels. For pure POPC membranes, the ion permeability properties are well established [28,29,59–61]:

$$P_K = 1 \times 10^{-14} \, m \, s^{-1}, \ P_{Cl} = 1 \times 10^{-13} \, m \, s^{-1}$$

 $P_H = 1 \times 10^{-9} \, m \, s^{-1}, \ P_{OH} = 1 \times 10^{-9} \, m \, s^{-1}$

We note that the significant difference in permeability values between the $\rm K^+/Cl^-$ ions and $\rm H^+/OH^-$ is typical of most ions for pure POPC bilayers [60,61]. The calculated changes in ion motion across the bilayer are translated into fluorescence time-lapse curves using the experimentally determined normalized calibration relationship for 0.03 mM HPTS at different pH values (Fig. S1). We note that this concentration of HPTS is sufficiently low such that there is no self-quenching of this dye [62]. The size of the vesicles for these calculations was obtained using DLS (Fig. S2A), with confirming evidence from cryo-EM (Fig. S2B).

We measured the fluorescence intensity changes of POPC vesicles prepared in a commonly used buffer (100 mM KCl, 100 mM HEPES, adjusted to pH 7.2 with 33 mM KOH) following the addition of 280 μ L 1 M KOH to the 2.5 mL vesicle solution, which raised the extra-vesicular pH to 12.6. These measurements exhibited excellent reproducibility between different sample batches (Fig. S3). As shown in Fig. 2, the calculated fluorescence increase curve based on the quantitative flux model (that is, equation (3) – (5)) is in excellent agreement with the experiment (R² = 0.97). Thus, the quantitative

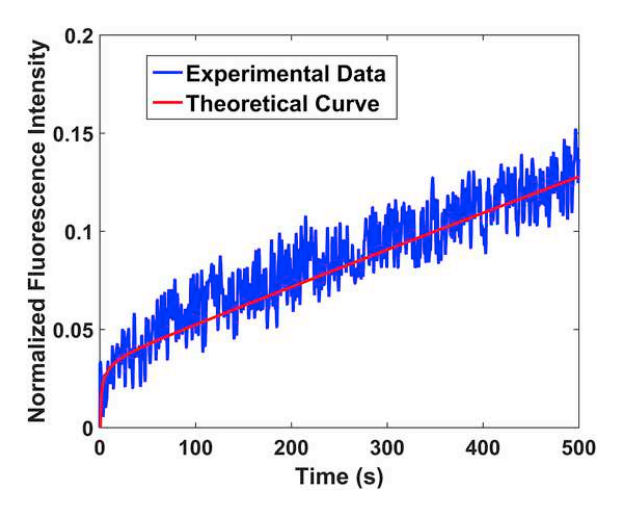


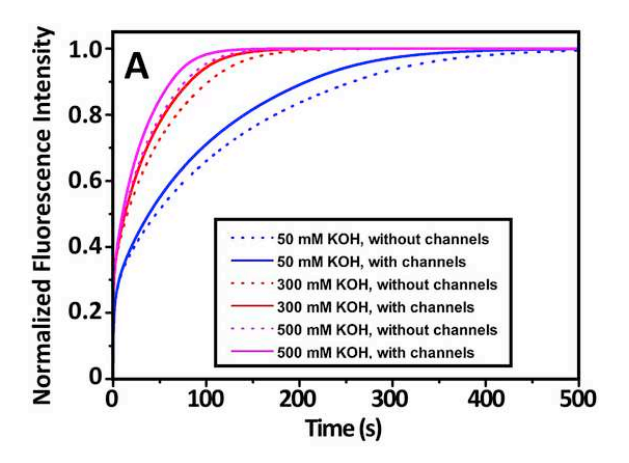
Fig. 2. Validation of the quantitative flux model. Shown are the experimental and theoretical results of the liposome assay using POPC vesicles without any channels following the addition of extra-vesicular KOH that produces an initial pH difference of 5.4.

model can indeed accurately describe the kinetics of ion transport in this assay.

3.2. Determining optimal conditions to improve the sensitivity of permeability measurements

Qualitative characterizations of ion channel permeability are usually obtained in liposome-based assays by comparing the kinetics of fluorescence changes in samples with or without channels. If the permeability of the channels is relatively low or only a few channels are present in the membrane, achieving reliable detection can be challenging since the lipid bilayer itself is permeable to most ions to various extents [29]. In addition, a less obvious characteristic of this assay that can significantly limit the detectability of channel permeability is the protonation/deprotonation of the buffering agent HEPES (or other buffering agents used).

To understand this effect, consider a vesicle with membrane-embedded channels exhibiting a vesicle-membrane permeability of $1.3 \times 10^{-14} \,\mathrm{m \, s^{-1}}$ for K^{+} , a typical case in many experiments [4]. With a buffer of 100 mM KCl and 10 mM HEPES (pH 5.3), as is common in many experiments, and an initial external KOH concentration of 300 mM, the quantitative flux model indicates that there is only a small difference in the fluorescence emission of HPTS entrapped inside vesicles with or without channels (that exhibit a K+-permeability of $1 \times 10^{-14} \, \text{m s}^{-1}$) (Fig. 3A, red lines). Such a difference cannot be easily resolved in experiments, as background noise is always present. Intuitively, it might be expected that a greater external KOH concentration of 500 mM that leads to a greater concentration gradient across the bilayer would yield a more unequivocal difference in these measurements. However, the quantitative flux model predicts an even smaller difference between the fluorescence curves in this case (Fig. 3A, pink lines). In fact, instead of increasing the KOH concentration, lowering the KOH concentration to 50 mM actually yields a greater difference in the kinetics measurements (Fig. 3A, blue lines). The reason for this counterintuitive outcome is that, although the greater concentration gradient across the bilayer indeed initially drives a greater amount of H⁺/OH⁻ transport through the membrane, it also shifts the intra-vesicular pH to a range of the HEPES titration curve



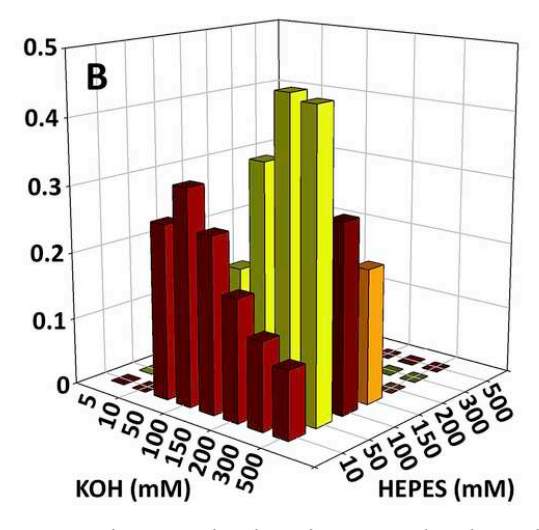


Fig. 3. Optimization of experimental conditions for measuring channel permeability. (A) Theoretical calculations of the difference in the fluorescence kinetics with (permeability of $1.3 \times 10^{-14} \, \text{m s}^{-1}$) or without (permeability of $1 \times 10^{-14} \, \text{m s}^{-1}$) membrane-embedded channels at different concentrations of extra-vesicular KOH (100 mM KCl, 10 mM HEPES, pH 5.3). (B) The magnitude of the area difference in the fluorescence intensity curves with/without channels from the calculations under different HEPES concentrations and final KOH concentrations with a channel vesicle K⁺-permeability of $1 \times 10^{-13} \, \text{m s}^{-1}$. All other ion permeability values are the same as in Fig. 1.

that is associated with a small slope, so a greater difference in the transported $\rm H^+/OH^-$ (between vesicles with channels and those without channels) is associated with a small change in pH (and thus fluorescence) (see Fig. S4). When the intra-vesicular pH approaches ~ 9 at which the HEPES is no longer an effective buffer, there is a sudden, significant difference in pH between the vesicles with channels and vesicles without channels. This, however, occurs in a pH range where the HPTS fluorescence essentially does not change (Fig. S4), and so the enlarged difference in intra-vesicular pH can no longer result in a significant change in fluorescence. By contrast, with 50 mM KOH, the intra-vesicular pH at the early phase of the fluorescence measurement (Fig. S4) is within the range of the HEPES titration curve that is associated with a larger slope, thus resulting in a greater difference in the intra-vesicular pH between vesicles with channels and those without.

To identify optimal conditions under which detection sensitivity is maximized, we systematically calculated the pre-

dicted effects of HEPES and KOH in a broad range of concentrations, assuming that with channels, the vesicle-membrane ion permeability increased from $1\times 10^{-14}~{\rm m~s^{-1}}$ to $1\times 10^{-13}~{\rm m~s^{-1}}$, which is similar to our experimental conditions (see below) (Fig. 3B). In this calculation, we used the integrated difference in fluorescence obtained with or without channels as the measure of detection sensitivity. We find that the dependence of detection sensitivity on the concentration of HEPES and that of external KOH is complex owing to the non-linear, sigmoidal relationship of HEPES concentration with solution pH and the lack of fluorescence change at pH values greater than 9 (as described above). Overall, these calculations predict that the concentrations at which this assay has the highest sensitivy are 50 mM HEPES and 300 mM KOH.

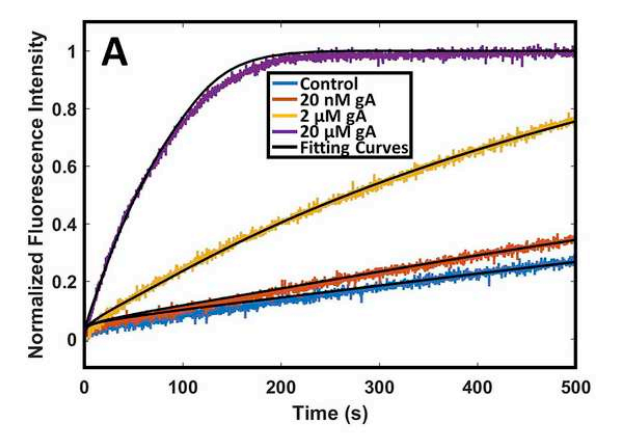
To validate the calculated predictions experimentally, we examined the detection sensitivity of a well-known small-peptide channel, gramicidin A (gA) [63]. This 15 amino acid peptide forms helical, cation-selective dimeric channels with a \sim 4 Å diameter lumen, with each monomer spanning only a single monolayer of the bilayer [64]. Previous studies showed that when gA is added to just one side of the membrane, there is a rapid rate of cross-bilayer channel formation (lasting 1–2 min), followed by a relatively stationary phase [65]. Therefore, this peptide can be simply added to the solution of preformed vesicles for the examination of stable permeability.

Fig. 4A shows the results obtained under the optimized conditions with gA concentrations of 20 nM to 20 μM . The channel activity can be clearly resolved even at concentrations of gA as low as 20 nM. In contrast, using buffer conditions typically employed by many (10 mM HEPES, 5 mM KOH) [51–54], channel activity is reliably detectable only when the concentration of gA is above 2 μM (Fig. 4B). Thus, the buffer conditions we optimized have improved the detection sensitivity of ion channel activity by 100-fold. We further note that, with our quantitative flux model, a direct measurement of the permeability of the vesicles can also be obtained, as detailed in the legend of Fig. 4.

We find that these optimal conditions are reasonably robust to the magnitude of ion permeability of the vesicles (Fig. S5), and so would be expected to be valid in most experiments. However, use of a different buffering agent other than HEPES would require a re-calculation using this model, since, as is clear from Fig. 3B, there are no clear-cut trends in detection sensitivity as a function of either HEPES or KOH concentrations.

3.3. Determining optimal conditions to measure ion selectivity ratios

To obtain the ion selectivity ratio of the channel, a typical approach is to compare the ionic permeabilities under conditions in which only the ions of interest are altered, while the number of channels in the membrane remains unchanged [67]. Here, the ability to detect small differences in the permeabilities of different ions is also highly dependent on the specific conditions. As shown in Fig. 5A, using the $\rm K^+/\rm Li^+$ selectivity of gA (~9/1) [68] as an example, we calculated the sensitivity needed to detect this difference in the liposome assay over a wide range of HEPES concentrations and external pH values. Again using the integrated fluorescence difference to determine sensitivity (of ion selectivity here), the most sensitive conditions are predicted to be 50 mM HEPES and 100 mM XOH (Fig. 5A; $\rm X = ion$ of interest). These predictions are validated by the experimental results shown in Fig. 5B. Fitting



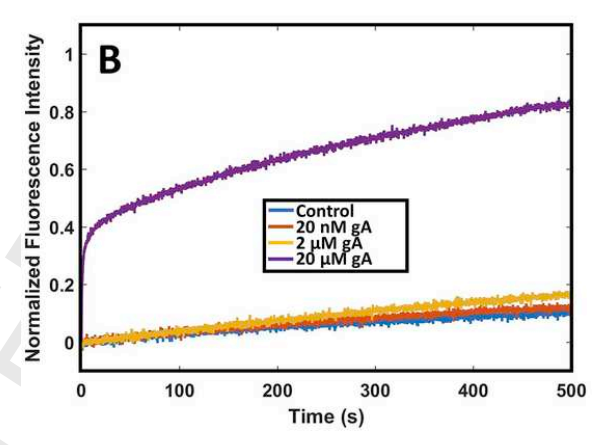


Fig. 4. Optimization of the experimental conditions improves the sensitivity of the assay by 100-fold. (A) The experimental data of the fluorescence intensity changes under optimal conditions of 50 mM HEPES and 300 mM external KOH with different concentrations of gA (100 mM KCl, pH 5.3). Fitting these data according to the calculations yield a permeability of, from bottom to top, $1 \times 10^{-14} \, \text{m s}^{-1}$, $4 \times 10^{-14} \, \text{m s}^{-1}$, $3 \times 10^{-13} \, \text{m s}^{-1}$, and $2.5 \times 10^{-12} \, \text{m s}^{-1}$, respectively. The non-linear dependence of the permeability on gA concentration is owing primarily to the well-known aggregation of gA in aqueous solution [66]. (B) The experimental data of the fluorescence intensity changes with different concentrations of gA with 10 mM HEPES and 5 mM external KOH (100 mM KCl, pH 5.3).

the experimental data to the quantitative flux model, we obtained values of the permeability of the vesicles to be 5 \times 10^{-14} m s $^{-1}$ for Li $^{+}$ and 4.2 \times 10^{-13} m s $^{-1}$ for K $^{+}$. Thus, the measured K $^{+}$ /Li $^{+}$ selectivity ratio for the gA channel is 8.4 \pm 0.8, in excellent agreement with the known ratio [68].

It is illustrative to consider this ion selectivity measurement under conditions which yield curves that, with simple inspection, would suggest a qualitatively incorrect ionic selectivity. Consider, for example, an experiment on the K^+/Li^+ selectivity of gA, but with 100 mM KCl in the initial vesicle solution (i.e., being present both inside and outside the vesicles) for each permeability measurement. As shown in Fig. 5C, if the ion selectivity is simply determined from an inspection of these curves, one would conclude that the permeability of Li^+ is greater than that of K^+ , which is clearly incorrect [68]. In this case, the presence of the initial concentration of K^+ in the experiments when the K^+ ion permeability was measured is expected to reduce the magnitude of the concentration gradient of K^+ following the extra-vesicular addition of KOH, thus resulting in a lower rate of fluorescence change than that with-

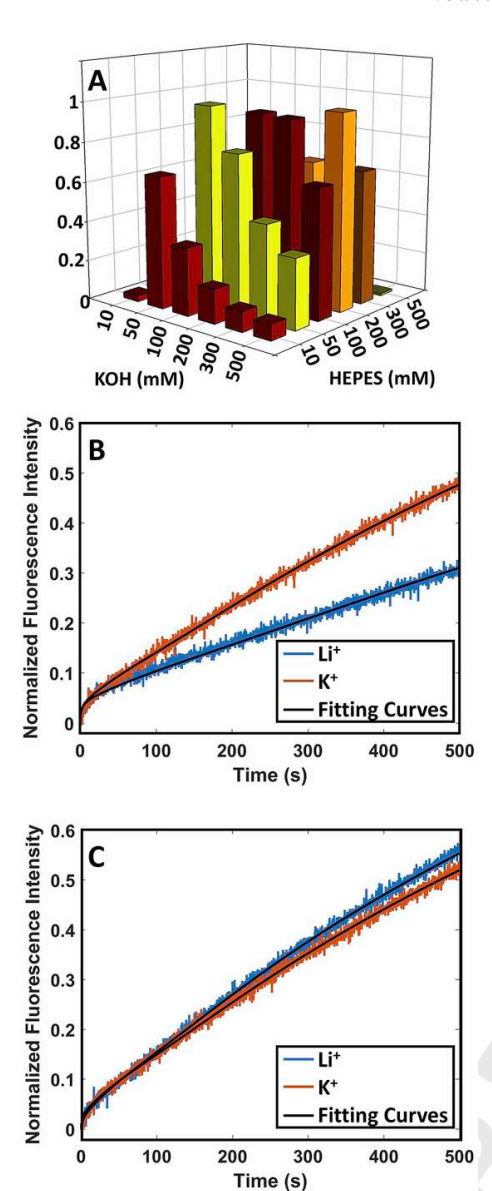


Fig. 5. Optimal conditions to detect differences in ion selectivity. (A) The calculated differences between the fluorescence curves of vesicles at different HEPES concentrations and KOH or LiOH concentrations with a vesicle permeability of $10^{-12}\,\mathrm{m}\,\mathrm{s}^{-1}$. (B) The experimental and theoretical fitting results of gA (40 nM) Li $^+/\mathrm{K}^+$ permeability under the optimized conditions of 50 mM HEPES, 100 mM NaCl, and 100 mM LiOH/KOH. The fits to the model yield a permeability of $5\times10^{-14}\,\mathrm{m}\,\mathrm{s}^{-1}$ for Li $^+$ and 4.2 \times 10 $^{-13}\,\mathrm{m}\,\mathrm{s}^{-1}$ for K $^+$, yielding a K $^+/\mathrm{Li}^+$ selectivity ratio of 8.4. (C) With 100 mM KCl present in the initial solutions of both experiments, inspection of the curves would suggest that Li $^+$ is more permeable than K $^+$, which is incorrect. However, when these conditions are included in the quantitative flux model, the correct K $^+/\mathrm{Li}^+$ ion selectivity ratio of 7.8 \pm 2.1 is obtained.

out the initial K^+ concentration. Thus, the seemingly lower selectivity of K^+ is owing to the lower concentration gradient of this ion, rather than the poorer selectivity of the channel for this ion.

However, even in this case, the quantitative flux model can still result in the correct K^+/Li^+ selectivity ratio of 7.8 \pm 2.1, if the initial concentration of KCl is used in the calculation (Fig. 5C). Thus, whether or not the experiments are performed under optimized conditions, fitting to the quantita-

tive flux model provides quantitatively accurate values of the selectivity ratios. In fact, under certain conditions, a completely surprising sequence of ion selectivity, even for simple synthetic ion channels that should more or less follow the hydration energy of the ions, could be found based on the qualitative evaluation of the curves (see Fig. S6). For such cases, the use of the quantitative flux model should help avoid incorrect assignments.

These examples clearly demonstrate that simply taking the kinetics of fluorescence change as a direct indicator for specific ion selectivity maybe unreliable, even when the curves are well resolved. As shown here, fitting to the quantitative flux model is necessary. However, we also note that, more frequently, the curves obtained under initial conditions cannot be sufficiently resolved (in the presence of experimental noise) to make reliable assignments. That is, with less optimal conditions, large differences in (fitted) permeability values are associated with relatively small differences in the kinetic curves, which compromise the ability to accurately quantify the differences in ion selectivity. Therefore, for a channel with unknown ion permeability properties, it is necessary to first conduct a series of experiments under different conditions so that the difference between fluorescence intensity changes are well resolved, and then fit the data with equation (1) to derive the ion selectivity of the channels.

4. Conclusions

The liposome-based assay is a simple and robust method to quantitatively determine ion transport properties of nano-channels. It can be performed in most laboratories without specialized instrumentation. However, as shown in this study, when the conditions used in the assay are less ideal or improper, the sensitivity of detecting channel permeability can be severely limited. More importantly, improper conditions can lead to wrongly assigned ionic selectivity sequences, and thus a fundamental mischaracterization of a basic function of the channel being examined.

We have shown that, by analyzing the data, under rigorously controlled experiments, according to the quantitative flux model, weakly permeable ion channels can now be resolved with optimal experimental conditions, and quantitatively accurate measures of ion selectivity can be unambiguously obtained. While it is possible to apply this vesicle-based assay with biological fluids, such as saliva and serum, a quantitative determination of the channel properties would require a full identification of the components of these complicated fluids, a rather challenging undertaking. Given the simplicity of the assay, especially the ease of controlling the experimental parameters, we anticipate that this ultrasensitive assay will find wide application in the quantitative characterization of ion channels, whether synthetic or biological.

CRediT authorship contribution statement

Yi Shen: Methodology, Software, Investigation. Yulong Zhong: Conceptualization, Validation. Fan Fei: Validation, Investigation. Jielin Sun: Project administration, Resources. Daniel M. Czajkowsky: Supervision, Writing - original draft. Bing Gong: Supervision, Writing - review & editing. Zhifeng Shao: Supervision, Writing - review & editing.

Declaration of competing interest

The authors declare that they have no known competing financial interests or personal relationships that could have appeared to influence the work reported in this paper.

Acknowledgments

This work was supported by grants from the National Key Research and Development Program of China (2018YFC1003501), the National Natural Science Foundation of China (Nos. 31670722, 81627801), the Science and Technology Commission of Shanghai Municipality (Nos. 17JC1400804, 18142202100), CAS Key Laboratory of Interfacial Physics and Technology (CASKL-IPT1702), and the US National Science Foundation (CHE-1905094).

Appendix A. Supplementary data

Supplementary data to this article can be found online at https://doi.org/10.1016/j.aca.2020.03.044.

Uncited reference

[66].

References

- [1] S P Adiga, C Jin, L A Curtiss, N A Monteiro-Riviere, R J Narayan, Nanoporous membranes for medical and biological applications, Wiley. Interdiscipl. Rev.: Nanomed. Nanobiotechnol 1 (5) (2009) 568–581.
- [2] B Yameen, M Ali, R Neumann, W Ensinger, W Knoll, O Azzaroni, Synthetic proton-gated ion channels via single solid-state nanochannels modified with responsive polymer brushes, Nano Lett. 9 (7) (2009) 2788–2793.
- [3] X Hou, W Guo, L Jiang, Biomimetic smart nanopores and nanochannels, Chem. Soc. Rev. 40 (5) (2011) 2385–2401.
- [4] X Zhou, G Liu, K Yamato, Y Shen, R Cheng, X Wei, W Bai, Y Gao, H Li, Y Liu, F Liu, D M Czajkowsky, J Wang, M J Dabney, Z Cai, J Hu, F V Bright, L He, X C Zeng, Z Shao, B Gong, Self-Assembling Subnanometer Pores with Unusual Mass-Transport Properties, 3, 2012, p. 949.
- [5] B Gong, Z Shao, Self-assembling organic nanotubes with precisely defined, sub-nanometer pores: formation and mass transport characteristics, Accounts Chem. Res. 46 (12) (2013) 2856–2866.
- [6] N Sakai, S Matile, Synthetic ion channels, Langmuir 29 (29) (2013) 9031–9040.
- [7] M H Patel, E Garrad, J W Meisel, S Negin, M R Gokel, G W Gokel, Synthetic ionophores as non-resistant antibiotic adjuvants, RSC Adv. 9 (2019) 2217.
- [8] W Song, M Kumar, Artificial water channels: toward and beyond desalination, Curr. Opin. Chem. Eng. 25 (2019) 9–17.
- [9] A J Helsel, A L Brown, K Yamato, W Feng, L Yuan, A J Clements, S V Harding, G Szabo, Z Shao, B Gong, Highly conducting transmembrane pores formed by aromatic oligoamide macrocycles, J. Am. Chem. Soc. 130 (47) (2008) 15784–15785.
- [10] J Geng, K Kim, J Zhang, A Escalada, R Tunuguntla, L R Comolli, F I Allen, A V Shnyrova, K R Cho, D Munoz, Y M Wang, C P Grigoropoulos, C M Ajo-Franklin, V A Frolov, A Noy, Stochastic transport through carbon nanotubes in lipid bilayers and live cell membranes, Nature 514 (7524) (2014) 612–615.
- [11] R H Tunuguntla, F I Allen, K Kim, A Belliveau, A Noy, Ultrafast proton transport in sub-1-nm diameter carbon nanotube porins, Nat. Nanotechnol. 11 (7) (2016) 639–644.
- [12] X Wei, G Zhang, Y Shen, Y Zhong, R Liu, N Yang, F Y Al-mkhaizim, M A Kline, L He, M Li, Z-L Lu, Z Shao, B Gong, Persistent organic nanopores amenable to structural and functional tuning, J. Am. Chem. Soc. 138 (8) (2016) 2749–2754.

- [13] S Howorka, Building membrane nanopores, Nat. Nanotechnol. 12 (7) (2017) 619–630.
- [14] R H Tunuguntla, R Y Henley, Y-C Yao, T A Pham, M Wanunu, A Noy, Enhanced water permeability and tunable ion selectivity in subnanometer carbon nanotube porins, Science 357 (6353) (2017) 792–796.
- [15] C Ren, F Chen, R Ye, Y S Ong, H Lu, S S Lee, J Y Ying, H Zeng, Molecular swings as highly active ion transporters, Angew. Chem., Int. Ed. Engl. 131 (2019) 8118.
- [16] T N Plank, L P Skala, J T Davis, Supramolecular hydrogels for environmental remediation: G4-quartet gels that selectively absorb anionic dyes from water, Chem. Commun. 53 (2017) 6235–6238.
- [17] P Xin, H Kong, Y Sun, L Zhao, H Fang, H Zhu, T Jiang, J Guo, Q Zhang, W Dong, C P Chen, Artificial K+ channels formed by pillararene-cyclodextrin hybrid molecules: tuning cation selectivity and generating membrane potential, Angew. Chem., Int. Ed. Engl. 58 (9) (2019) 2779–2784.
- [18] W Si, P Xin, Z Li, J Hou, Tubular unimolecular transmembrane channels: construction strategy and transport activities, Acc. Chem. Res. 48 (2015) 1612–1619.
- [19] S P Zheng, Y H Li, J J Jiang, A van der Lee, D Dumitrescu, M Barboiu, Self-Assembled columnar triazole quartets: an example of synergistic hydrogen-bonding/anion–π interactions, Angew. Chem., Int. Ed. Engl. 131 (2019) 12165.
- [20] X Wu, J R Small, A Cataldo, A M Withecombe, P Turner, P A Gale, Voltage-Switchable HCl transport enabled by lipid headgroup, Angew. Chem., Int. Ed. Engl. 131 (2019) 15286.
- [21] A Nakano, Q Xie, J V Mallen, L Echegoyen, G W Gokel, Synthesis of a membrane-insertable, sodium cation conducting channel: kinetic analysis by dynamic sodium-23 NMR, J. Am. Chem. Soc. 112 (3) (1990) 1287–1289.
- [22] T M Fyles, T D James, K C Kaye, Activities and modes of action of artificial ion channel mimics, J. Am. Chem. Soc. 115 (26) (1993) 12315–12321.
- [23] R H Ashley, Ion Channels: A Practical Approach, IRL Press at Oxford University Press, 1995.
- [24] P H Schlesinger, R Ferdani, J Liu, J Pajewska, R Pajewski, M Saito, H Shabany, G W Gokel, SCMTR: A chloride-selective, membrane-anchored peptide channel that exhibits voltage gating, J. Am. Chem. Soc. 124 (9) (2002) 1848–1849.
- [25] W Walz, A A Boulton, G B Baker, Patch-Clamp Analysis: Advanced Techniques, Humana Press, 2002.
- [26] C A Schalley, Analytical Methods in Supramolecular Chemistry, Wiley, 2012.
- [27] G W Gokel, S Negin, Synthetic ion channels: from pores to biological applications, Accounts Chem. Res. 46 (12) (2013) 2824–2833.
- [28] J W Nichols, D W Deamer, Net proton-hydroxyl permeability of large unilamellar liposomes measured by an acid-base titration technique, Proc. Natl. Acad. Sci. U. S. A. 77 (4) (1980) 2038–2042.
- [29] D W Deamer, J W Nichols, Proton-hydroxide permeability of liposomes, Proc. Natl. Acad. Sci. U. S. A. 80 (1) (1983) 165–168.
- [30] N Busschaert, R B Elmes, D D Czech, X Wu, I L Kirby, E M Peck, K D Hendzel, S K Shaw, B Chan, B D Smith, K A Jolliffe, P A Gale, Thiosquaramides: pH switchable anion transporters, Chem. Sci. 5 (9) (2014) 3617–3626.
- [31] M M Daschbach, S Negin, L You, M Walsh, G W Gokel, Aggregation and supramolecular membrane interactions that influence anion transport in tryptophan-containing synthetic peptides, Chemistry 18 (24) (2012) 7608–7623.
- [32] J T Davis, P A Gale, O A Okunola, P Prados, J C Iglesias-Sanchez, T Torroba, R Quesada, Using small molecules to facilitate exchange of bicarbonate and chloride anions across liposomal membranes, Nat. Chem. 1 (2) (2009) 138–144.
- [33] Y J Jeon, H Kim, S Jon, N Selvapalam, D H Oh, I Seo, C S Park, S R Jung, D S Koh, K Kim, Artificial ion channel formed by cucurbit[n]uril derivatives with a carbonyl group fringed portal reminiscent of the selectivity filter of K+ channels, J. Am. Chem. Soc. 126 (49) (2004) 15944–15945.
- [34] M S Kaucher, M Peterca, A E Dulcey, A J Kim, S A Vinogradov, D A Hammer, P A Heiney, V Percec, Selective transport of water mediated by porous dendritic dipeptides, J. Am. Chem. Soc. 129 (38) (2007) 11698–11699.
- [35] S K Ko, S K Kim, A Share, V M Lynch, J Park, W Namkung, W Van Rossom, N Busschaert, P A Gale, J L

- Sessler, I Shin, Synthetic ion transporters can induce apoptosis by facilitating chloride anion transport into cells, Nat. Chem. 6 (10) (2014) 885–892.
- [36] A Kocer, M Walko, W Meijberg, B L Feringa, A light-actuated nanovalve derived from a channel protein, Science 309 (5735) (2005) 755–758.
- [37] Y Le Duc, M Michau, A Gilles, V Gence, Y M Legrand, A van der Lee, S Tingry, M Barboiu, Imidazole-quartet water and proton dipolar channels, Angew. Chem. 50 (48) (2011) 11366–11372.
- [38] M Ma, A Paredes, D Bong, Intra- and intermembrane pairwise molecular recognition between synthetic hydrogen-bonding phospholipids, J. Am. Chem. Soc. 130 (44) (2008) 14456–14458.
- [39] D Milano, B Benedetti, M Boccalon, A Brugnara, E Iengo, P Tecilla, Anion transport across phospholipid membranes mediated by a diphosphine-Pd(II) complex, Chem. Commun. 50 (65) (2014) 9157–9160.
- [40] J M Moszynski, T M Fyles, Mechanism of ion transport by fluorescent oligoester channels, J. Am. Chem. Soc. 134 (38) (2012) 15937–15945.
- [41] F Otis, C Racine-Berthiaume, N Voyer, How far can a sodium ion travel within a lipid bilayer?, J. Am. Chem. Soc. 133 (17) (2011) 6481–6483.
- [42] J M Priegue, J Montenegro, J R Granja, Single-nucleotide-resolution DNA differentiation by pattern generation in lipid bilayer membranes, Small 10 (18) (2014) 3613–3618.
- [43] S Turkyilmaz, W H Chen, H Mitomo, S L Regen, Loosening and reorganization of fluid phospholipid bilayers by chloroform, J. Am. Chem. Soc. 131 (14) (2009) 5068–5069.
- [44] H Valkenier, N Lopez Mora, A Kros, A P Davis, Visualization and quantification of transmembrane ion transport into giant unilamellar vesicles, Angew. Chem. 54 (7) (2015) 2137–2141.
- [45] C P Wilson, S J Webb, Palladium(II)-gated ion channels, Chem. Commun. (34) (2008) 4007–4009.
- [46] H Y Zha, B Shen, K H Yau, S T Li, X Q Yao, D Yang, A small synthetic molecule forms selective potassium channels to regulate cell membrane potential and blood vessel tone, Org. Biomol. Chem. 12 (41) (2014) 8174–8179.
- [47] C Hannesschlaeger, T Barta, H Pechova, P Pohl, The effect of buffers on weak acid uptake by vesicles settings, Biomolecules 9 (2) (2019) 63.
- [48] M Zheng, T M Fyles, Properties of liposomes containing natural and synthetic lipids formed by microfluidic mixing, Eur. J. Lipid Sci. Technol. 120 (2018) 1700347.
- [49] D Jaeger, J Ranu, Encyclopedia of Computational Neuroscience, Springer, New York, 2015.
- [50] J-Y Winum, S Matile, Rigid push pull oligo (p-phenylene) rods: depolarization of bilayer membranes with negative membrane potential, J. Am. Chem. Soc. 121 (34) (1999) 7961–7962.
- [51] R E Dawson, A Hennig, D P Weimann, D Emery, V Ravikumar, J Montenegro, T Takeuchi, S Gabutti, M Mayor, J Mareda, C A Schalley, S Matile, Experimental evidence for the functional relevance of anion-π interactions, Nat. Chem. 2 (7) (2010) 533-538
- [52] A V Jentzsch, D Emery, J Mareda, S K Nayak, P Metrangolo, G Resnati, N Sakai, S Matile, Transmembrane anion transport mediated by halogen-bond donors, 3 (2012) 905.
- [53] S Benz, M Macchione, Q Verolet, J Mareda, N Sakai, S Matile, Anion transport with chalcogen bonds. J. Am. Chem. Soc. 138 (29) (2016) 9093–9096.
- [54] H J Clarke, E N Howe, X Wu, F Sommer, M Yano, M E Light, S Kubik, P A Gale, Transmembrane fluoride transport: direct measurement and selectivity studies, J. Am. Chem. Soc. 138 (50) (2016) 16515–16522.
- [55] N R Clement, J M Gould, Pyranine (8-hydroxy-1,3,6-pyrenetrisulfonate) as a probe of internal aqueous hydrogen ion concentration in phospholipid vesicles, Biochemistry 20 (6) (1981) 1534–1538.
- [56] M Rossignol, P Thomas, C Grignon, Proton permeability of liposomes from natural phospholipid mixtures, Biochim. Biophys. Acta Biomembr. 684 (2) (1982) 195–199.
- [57] N Opitz, D W Lubbers, A correction method for ionic strength-independent fluorescence photometric pH measurement, Adv. Exp. Med. Biol. 169 (1984) 007, 012
- [58] R N Roy, L N Roy, S Ashkenazi, J T Wollen, C D Dunseth, M S Fuge, J L Durden, C N Roy, H M Hughes, B T Morris, Buffer standards for pH measurement of N-(2-Hydroxyethyl) piperazine-N'-2-ethanesulfonic acid (HEPES) for I = 0.16 mol·kg-1 from 5 to 55° C, J. Solut. Chem. 38 (4) (2009) 449-458.

- [59] Y Nozaki, C Tanford, Proton and hydroxide ion permeability of phospholipid vesicles, Proc. Natl. Acad. Sci. U. S. A. 78 (7) (1981) 4324–4328.
- [60] D W Deamer, Proton permeation of lipid bilayers, J. Bioenerg. Biomembr. 19 (5) (1987) 457–479.
- [61] W R Perkins, D S Cafiso, An electrical and structural characterization of H+/ OH- currents in phospholipid vesicles, Biochemistry 25 (8) (1986) 2270–2276.
- [62] N Yonet-Tanyeri, R C Evans, H Tu, P V Braun, Molecular transport directed via patterned functionalized surfaces, Adv. Mater. 23 (15) (2011) 1739–1743.
- [63] N Foundation, Gramicidin and Related Ion Channel-Forming Peptides, Wiley, 2008.
- [64] D A Kelkar, A Chattopadhyay, The gramicidin ion channel: a model membrane protein, Biochim. Biophys. Acta Biomembr. 1768 (9) (2007) 2011–2025.
- [65] A M O'Connell, R E Koeppe, O S Andersen, Kinetics of gramicidin channel formation in lipid bilayers: transmembrane monomer association, Science 250 (4985) (1990) 1256–1260.
- [66] G Kemp, C Wenner, Solution, interfacial, and membrane properties of gramicidin A, Arch. Biochem. Biophys. 176 (2) (1976) 547–555.
- [67] N Sakai, S Matile, The determination of the ion selectivity of synthetic ion channels and pores in vesicles, J. Phys. Org. Chem. 19 (8–9) (2006) 452–460.
- [68] P Prangkio, D K Rao, K D Lance, M Rubinshtein, J Yang, M Mayer, Self-assembled, cation-selective ion channels from an oligo (ethylene glycol) derivative of benzothiazole aniline, Biochim. Biophys. Acta Biomembr. 1808 (12) (2011) 2877–2885.